Eur Biophys J (1984) 11:43–50

European Biophysics Journal

Flux measurement in single cells by fluorescence microphotolysis

R. Peters

Max-Planck-Institut für Biophysik, Kennedy-Allee 70, D-6000 Frankfurt 70, Federal Republic of Germany

Received March 6, 1984/Accepted May 14, 1984

Abstract. Fluorescence microphotolysis – widely employed for diffusion studies – can be used to measure transfer (flux) of fluorescent solutes through membranes in single cells and organelles. This article analyses the methodological basis of flux measurements, provides experimental tests, and discusses potential applications. The principle of the method is to equilibrate cells, organelles or vesicles with a fluorescent solute, to deplete the interior of individual cells etc. of fluorescene by the pulse of a high-intensity microbeam, and to monitor influx of solute by microfluorometry. Simple equations are given and a computer curve fitting program is described by which rate constants of influx and membrane permeability coefficients can be derived from fluorescence measurements. The permeability of individual "leaky" human erythrocyte ghosts to fluorescein-isothiocyanate-labelled bovine serum albumin has been measured under various conditions. Multiple exposure to the high-intensity microbeam had no effect on permeability within experimental error. Flux measurements have been also performed on individual vesicles of 1–2 μm radius which had been derived from ghosts. The potential application of the method to sub-lightmicroscopic vesicles and to organelles within living cells is discussed.

Key words: Flux measurement, photobleaching, fluorescence microphotolysis, erythrocyte

Introduction

The transfer of solutes across membranes is a crucial parameter in many cellular functions. Therefore, a large number of methods have been devised for following solute transfer either continuously – e.g., by ion-selective electrodes or fluorometry – or discontinuously – e.g., by rapid separation techniques (for details or review see Christensen 1975; Eidelman and Cabantchik 1980; Halestrap and McCivan 1979; Pfaff and Klingenberg 1968; Wohlhueter et al. 1978). In addition, the theory of transfer kinetics has been worked out for many special cases involving passive or active (i.e., energy-consuming) mechanisms (Kotyk and Janáçek 1970; Schulz 1980). This article describes yet another method for the measurement of transfer through membranes that is characterized, however, by some unique properties. It can be applied to single, normal-sized cells or single isolated cell organelles; the permeability of organelle membranes can be measured even in situ, i.e., within the living cell; time-resolution is high (ms), and sensitivity large. The method is based on fluorescence microphotolysis ("photobleaching") and is therefore restricted to fluorescent solutes.

Fluorescence microphotolysis makes use of a property of many fluorescent chromophores: exposed to high light intensities, these chromophores are photochemically modified and become non-fluorescent. This has been known for a long time as "fading" or "photobleaching". In 1974 it was shown (Peters et al. 1974) that photobleaching – if combined with microfluorometry – can be employed for diffusion measurements at the spatial resolution of the light microscope. In subsequent years the method was considerably improved (Edidin et al. 1976; Jacobson et al. 1976; Axelrod et al. 1976) and a number of special versions were described (Smith and McConnell 1978; Koppel 1979; Thompson et al. 1981; Peters et al. 1981; Smith et al. 1981; Lanni and Ware 1982; Davoust et al. 1982). Fluorescence microphotolysis has been mainly used to measure translational diffusion coefficients of proteins and lipids in various types of membranes (for review see Cherry 1979; Peters 1981; Koppel 1983; Vaz et al. 1982; Axelrod 1983; Peters 1983a). The major objective of those studies was to elucidate the structural basis and the

Abbreviation: FITC-BSA = fluorescein isothiocyanate-labeled bovine serum albumin

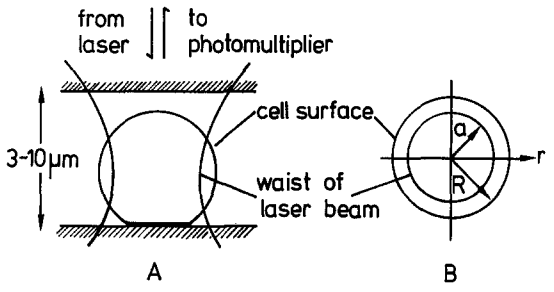

Fig. 1A and B. The basic concept of flux measurement by fluorescence microphotolysis. **A** View from the side. Cells are incubated with a fluorescent solute. A layer of the cell suspension not much thicker than the cells is enclosed between a glass slide and a cover slip. In a fluorescence microscope a single cell is brought into focus and illuminated by an attenuated laser beam. The beam, in the focal plane, covers a major part of the cross-section of the cell. Using a high-intensity laser pulse, the interior of the cell is depleted of fluorescence. Employing the initial low excitation energy, fluorescence recovery is monitored and used to derive the rate constant of influx. **B** View from above. The radius of the cell is denoted as R, the radius of the illuminated area in the focal plane is a

physiological implication of molecular motion in cell membranes.

Recently we have employed fluorescence microphotolysis for studies of solute transport into single isolated liver cell nuclei (Peters 1983b). In the present article the methodological basis of flux measurements by fluorescence microphotolysis is analysed. Simple equations are derived relating the time-course of fluorescence recovery to the rate constant of influx and to the membrane permeability coefficient. Curve fitting by computer is described. As an experimental test the influx of fluoresceinisothiocyanate-labelled bovine serum albumin (FITC-BSA) into human erythrocyte ghosts and small vesicles has been measured. The characteristics of the method and its potential usage are discussed.

Experimental

The principle of flux measurement by fluorescence microphotolysis

Cells are equilibrated with a fluorescent solute. As indicated in Fig. 1A a thin layer of the cell suspension is enclosed between a glass slide and a cover slip. On the stage of a microscope equipped for fluorescence microphotolysis a cell is brought into focus and illuminated by an attenuated laser beam. In the Appendix it is shown that neither the size nor the intensity profile of the laser beam is critical. The optimum signal quality, however, is obtained if the beam covers a major part of the cross-section of the cell, as indicated in Fig. 1. Fluorescence is measured. The intensity of the beam is suddenly increased by several orders of magnitude in order to photolyse the fluorophores and render them non-fluorescent in a short time. The initial low beam power is restored and fluorescence again mesured. The time-course of fluorescence recovery, under many experimental conditions (specified in the Appendix), is only determined by the permeation of solute from the surroundings into the cell. If the solute is uncharged and penetrates the cell membrane by a passive, diffusional mechanism the time-course of intracellular fluorescence is given by:

$$\ln \frac{1}{F(\infty) - F(t)} = \ln \frac{1}{F(\infty) - F(0)} + kt, \qquad (1)$$

where $F(0)$, $F(t)$, and $F(\infty)$ is intracellular fluorescence immediately, at time t, and at infinite time after photolysis, respectively, and k is the rate constant of influx. In analogy to diffusion measurements by fluorescence microphotolysis a "mobile fraction" of the solute is defined (Axelrod et al. 1976) as:

$$R_M = \frac{F(\infty) - F(0)}{F(-) - F(0)} \qquad (2)$$

where $F(-)$ is intracellular fluorescence before photolysis. Equation 1 and other equations are derived in the Appendix.

Material

FITC-BSA was obtained from Sigma (St. Louis, Alabama, USA) und tested for purity by gel electrophoresis. The degree of labelling was 9.9 moles of fluorescein per mole of albumin.

Preparation of ghosts

Ghosts were prepared according to Dodge et al. (1963). Human blood (group 0, Rh+) was obtained from a blood bank. Erythrocytes were washed three times in isotonic saline. The packed erythrocytes were suspended in a 40-fold volume of ice-cold 7 mM sodium phosphate buffer, pH 7.6, and washed four times in the same buffer to yield a white pellet of erythrocyte ghosts.

Preparation of specimen for flux measurements

FITC-BSA was dissolved in 7 mM sodium phosphate buffer, pH 7.6, at a final concentration of 19 µM. The FITC-BSA solution was mixed with the ghost sus-

pension at a ratio of 9/1 vol/vol. After 30 min, 1 µl of the FITC-BSA/ghost suspension was placed on a carefully cleaned glass slide and covered by a 18-mm × 18-mm cover slip. The suspension spread spontaneously between slide and cover slip to yield a layer of about 3 µm average thickness. The specimen was sealed at the edges of the cover slip with silicon grease of medium viscosity. In some of the experiments, the FITC-BSA/ghost suspension was diluted with distilled water to reduce the buffer concentration to 1 mM.

Ghost vesicles were prepared by syringing a FITC-BSA/ghost suspension through a no. 27 needle. The procedure yielded a suspension of vesicles very heterogeneous in size. For flux measurements vesicles with diameters of 1–2 µm were selected in the specimen under the microscope. The vesicle diameter was measured by means of a calibrated scale in the ocular lens.

Instrumentation

Most of the equipment used in this study for fluorescence microphotolysis has been described previously (Peters and Richter 1981). A fast scanning stage (Zeiss) that allows movement of the specimen in the focal plane in steps of 0.25 µm was added to the microscope. The step rate could be adjusted from 0/s to a maximum of 10,000/s. Furthermore, a computer (Digital Equipment, model MINC 23) was employed for plotting data in real time and for evaluating them under graphic visualization. The 4765 Å laser line of an argon laser was used at about 200 mW. A 100× oil-immersion objective lens (n.a. 1.30) was employed. In measurements of intact ghosts the illuminated area had a radius of 2.0 µm; in measurements of ghost vesicles a 1.0-µm radius was used. In both cases the illuminated area had a uniform intensity and the intensity ratio of photolysing to measuring beam was approximately 10^5. The photolysis time was usually $\frac{1}{8}$ s. Fluorescence was measured employing a photometric attachment to the microscope (Zeiss). This device incorporates an adjustable diaphragm positioned at an image plane in front of the photomultiplier. The diaphragm is crucial because it permits fluorescence originating from the focal plane to reach the photomultiplier while rejecting much of the fluorescence from other points of the specimen (see Koppel et al. 1976 for a quantitative analysis). Profiles of fluorescence intensity of individual ghosts were obtained with an illuminated area of 0.5 µm. A ghost was moved on a linear pathway through the illuminated area at a speed of about 1.5 µm/s while fluorescence was measured at a sampling time of 200 ms. Then, the ghost was positioned centrally in respect of the illuminated area and photolysed for 4 s. Scanning was repeated at various times after photolysis. In all experiments the temperature was 22°–23° C.

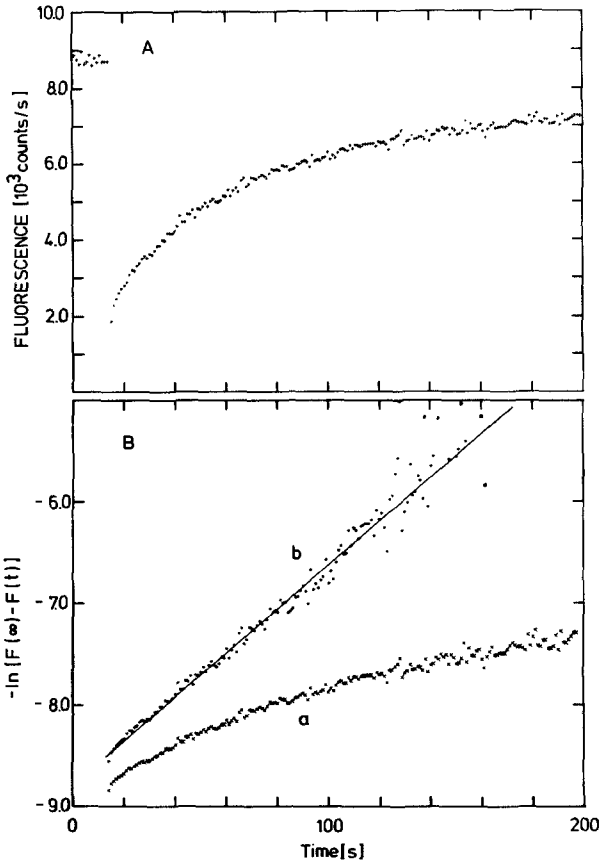

Fig. 2A and B. Influx of fluorescein isothiocynate-labelled bovine serum albumin into a "leaky" human erythrocyte ghost (concentration of albumin was 17.1 µM). **A** Raw data are given as counts/s versus time. The three consecutive steps of the experiment can be recognized: measurement of fluorescence $F(-)$ before photolysis, reduction of fluorescence by photolysis to $F(0)$, and measurement of $F(t)$. At large times $F(t)$ approaches asymptotically $F(\infty)$. **B** Data are evaluated by plotting $\ln [1/(F(\infty) - F(t)]$ versus time. In an initial plot (curve a) $F(\infty)$ is set equal to $F(-)$. Then, a search is made by computer for the $F(\infty)$-value that yields optimum linearity, i.e., smallest chi-square (curve b). The slope of the best fit is equal to the rate constant of influx. The fact that $F(\infty)$ and $F(-)$ are not identical indicates that part of the solute is immobilized presumably by adsorption to the membrane

Results

The data on influx of FITC-BSA into ghosts and ghost vesicles are presented in Figs. 2–4 and Table 1. Figure 2 gives a typical example of flux data when ghosts were suspended in 7 mM sodium phosphate buffer, pH 7.6. In the upper panel (Fig. 2A) the raw

Table 1. Permeability of human erythrocyte ghosts to fluorescein isothiocyanate-labelled bovine serum albumin as measured by fluorescence microphotolysis[a]

Medium	k (1)[b] s^{-1}	P[c] 10^{-8} cm/s	R_M[d]	k (2)/k (1)[b]	k (3)/k (1)[b]	n
7 mM sodium phosphate buffer, pH 7.6	0.0134 ± 0.0093	12.46 ± 8.46	0.71 ± 0.10			21
1 mM sodium phosphate buffer, pH 7.6	0.1595 ± 0.1269	148.3 ± 118.0	0.83 ± 0.14	1.04 ± 0.14	1.06 ± 0.16	17

[a] Mean ± SD of n measurements
[b] k (1), k (2), and k (3) are rate constants derived from the 1st, 2nd, and 3rd measurement, respectively, of the same ghost
[c] Permeability coefficient according to Eq. (6)
[d] Mobile fraction according to Eq. (2)

data are shown. The three steps of the experiment – measurement of fluorescence F(−) before photolysis; photolysis and reduction of fluorescence to F(0); and measurement of $F(t)$ – are clearly apparent. In the lower panel (Fig. 2B) the data have been transformed according to Eq. (1) and plotted as ln $1/[F(\infty)-F(t)]$ versus time. In an initial plot $F(\infty)$ was set equal to $F(-)$, which yielded curve a in Fig. 2B. Then, a search was made by computer (see Appendix) for the $F(\infty)$-value, which yielded maximum linearity, i.e., smallest chi-square. The result is curve b in Fig. 2B, in which the experimental data have been superimposed with the fitted curve. From the fitted curve the following values were derived: $F(-)$ = 8,761 counts/s, $F(0)$ = 2,212 counts/s, $F(\infty)$ = 7,031 counts/s, mobile fraction $R_M = 0.74$, $k = 0.0219\ s^{-1}$, permeability coefficient $P = 20.4 \times 10^{-8}$ cm/s, and reduced chi-square = 0.59.

Mean values and standard deviations of k, P, and R_M obtained in measurements of 21 individual ghosts are given in Table 1. The permeability coefficient of $(12.4 \pm 8.6) \times 10^{-8}$ cm/s is in reasonable agreement with previous measurements of the permeability of ghosts to dextrans (Peters 1983b). For a dextran of 62,000 dalton molecular mass, for instance, a permeability coefficient of 78×10^{-8} cm/s was measured.

The measurements indicate the presence of an "immobile" fraction of the solute. A simple explanation for this feature would be that FITC-BSA has a tendency to adsorb to the erythrocyte membrane. This hypothesis is supported by intensity profiles obtained from individual ghosts (Fig. 3). Before photolysis, fluorescence of the ghost is larger than that of the surroundings, indicating an accumulation of FITC-BSA by the ghost. After photolysis, ghost fluorescence depends on time, as expected. The profiles are flat (i.e., parallel to the time-axis) both inside and outside the ghost because the ghosts assume a disc-like shape in the thin fluid layer between slide and cover slip and because both the internal and external phase is in diffusional equilibrium at all times.

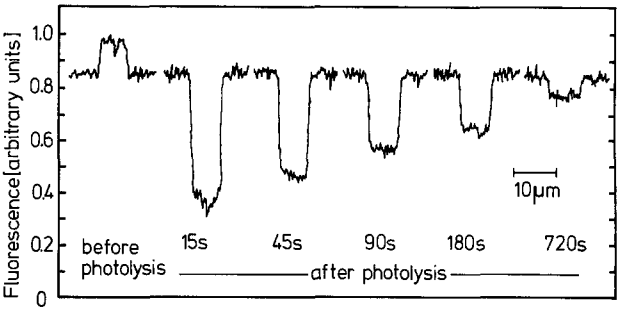

Fig. 3. Fluorescence intensity profiles of a ghost suspended in a 17.1 µM solution of fluorescein isothiocyanate-labelled bovine serum albumin. Before photolysis fluorescence of the ghost is larger than that of the surroundings indicating adsorption of albumin to the membrane. After photolysis influx of albumin gives rise to a time-dependent increase in intracellular fluorescence. The intensity profile is essentially flat both inside and outside the ghost, showing that a concentration gradient exists only across the membrane

The permeability properties of ghosts at a smaller buffer concentration (1 mM) are listed in Table 1. In these experiments individual ghosts were subjected to three consecutive measurements, allowing for complete equilibration between measurements. The rate constants derived from the first, second, and third measurement are denoted as $k(1)$, $k(2)$, and $k(3)$, respectively. In Table 1 $k(1)$ and the ratios $k(2)/k(1)$ and $k(3)/k(1)$ – determined for each ghost separately and then averaged – are given. This procedure shows that the uncertainty in repeated measurements is about ± 15%. Furthermore, no differences were detected between $k(1)$, $k(2)$, and $k(3)$ within the uncertainty limit. The absolute values of k are about 10-fold larger at 1 mM than at 7 mM buffer concentration. This observation is in agreement with recent reports by Lieber and Steck (1982), showing that the permeability of ghosts to hydrophilic solutes depends sensitively on ionic strength.

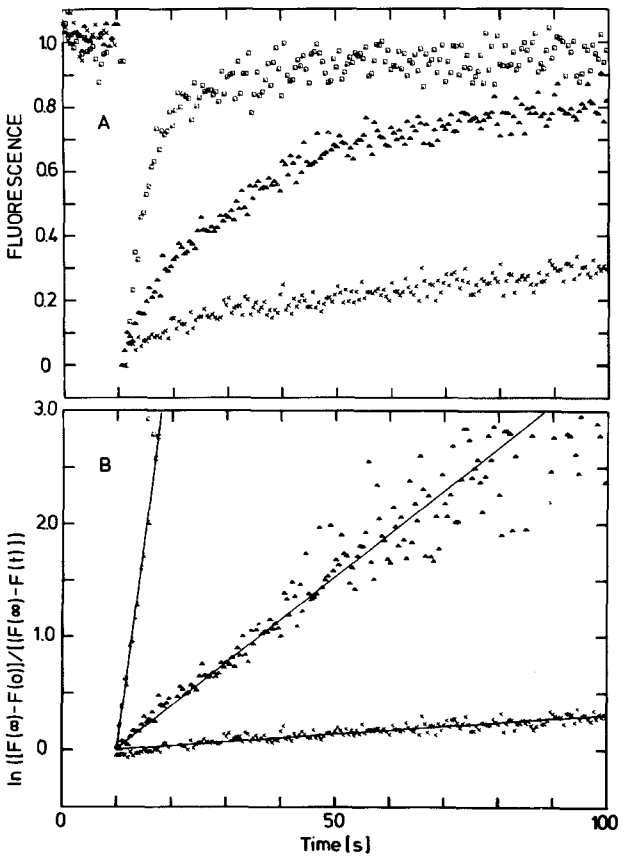

Fig. 4A and B. Flux measurements on small vesicles. Vesicles of 1–2 μm radius were derived from erythrocyte ghosts and influx of fluorescein isothiocyanate-labelled bovine serum albumin was measured. Rate constants were found to vary largely from vesicle to vesicle. As example measurements on three individual vesicles are shown (**A**: raw data in normalized form, i.e., $[F(t) - F(0)]/[F(-) - F(0)]$ versus time, **B**: semilogarithmically transformed data similar to Fig. 2B but in normalized form). The figure is to show that flux data of acceptable quality can be obtained from single small vesicles

In measurements on small ghost-derived vesicles both the rate constants and permeability coefficients were found to vary largely. In measurements of 17 individual vesicles ranging in radius from 1.0 to 2.1 μm, the rate constants varied from 0.0024 s^{-1} to 0.394 s^{-1}. Permeability coefficients showed a similarly large scatter: (2.9–163.3) × 10^{-8} cm/s. Possibly, the shearing procedure that was used to generate the vesicles creates additional leaks in the membrane. However, a different explanation for the extreme variability can not be ruled out and remains to be explored. The number of leaks per ghost may be so small (Lieber and Steck 1982) that vesicles with 0,1,2... leaks are produced. Figure 4 gives three examples of flux measurements. These records demonstrate that data of sufficient quality can be obtained in measurements of single small vesicles.

Discussion

An obvious advantage of the method described is its high resolution in both time and space. Time resolution is essentially limited by photolysis. The photolysis time should be short compared to the relaxation time of influx. With mechanical shutters the shortest photolysis time is close to 1 ms, so that membrane transport processes of about 10 ms relaxation time or longer can be measured. It has been shown, however, that acousto-optical modulation in combination with signal averaging can push the time resolution of photobleaching measurements into the μs-time range (Johnson and Garland 1981).

The spatial resolution of flux measurements by fluorescence microphotolysis is not limited by optical diffraction. As discussed in the Appendix the kinetics of fluorescence recovery are independent of the size of the illuminated area provided that diffusion is much faster than membrane transport. Equation (12) shows, however, that contrast is rapidly lost with increasing radius a of the illuminated area, i.e., $F(0)/F(\infty)$ approaches 1.0 for large a. This effect could be balanced by placing more than just one vesicle into the illumination area. Since it is furthermore essential to keep diffusion times short, the illuminated area should assume a slit-like geometry. We suggest measuring membrane transport in sub-lightmicroscopic vesicles by employing thin layers of relatively densely packed vesicles and stripes or grids as geometry of the illuminated area. From the technical point of view this procedure is identical to pattern photobleaching inaugurated by Smith and McConnell (1978) for diffusion measurements.

Flux measurements by fluorescence microphotolysis require extremely small numbers of cells and solute molecules. This may be crucial when rare molecular species are to be studied.

The method is restricted to fluorescent and irreversibly bleachable solutes. The smallest molecules fulfilling these conditions possibly are certain rare-earth and heavy-metal ions (e.g., Parker 1968). More typically, organic fluorophores such as carbocyanine dyes (Sims et al. 1974) or fluorescently labelled compounds such as certain anions (Eidelman and Cabantchik 1980) and a variety of macromolecules will be involved.

Radiation-induced artefacts are a potential complication in all types of photobleaching experiments. The matter has been studied rather extensively with respect to diffusion measurements (Axelrod 1977; Jacobsen et al. 1978; Nigg et al. 1979; Sheetz and Koppel 1979; Wolf et al. 1980). From these studies some general aspects have emerged which may also be valid for flux measurements. Heating and photochemical cross-linking are the most obvious dangers

associated with high-intensity irradiation of fluorescently labelled molecules. Heating, among other parameters, depends on the concentration of fluorophores which, however, can be varied within rather wide limits. Photochemical effects depend in a complicated fashion on many parameters two of which are intensity and dose of irradiation. The available evidence suggests that at the specific conditions employed in fluorescence microphotolysis cross-linking is not a problem. Furthermore, cross-linking is prevented or quickly reversed by glutathione and certain other reductants (Sheetz and Koppel 1979) which are physiological constitutents of living cells. In the present experiments we have checked for radiation-induced artefacts by repetitive photolysis of individual ghosts. No effect on rate constants has been disclosed within experimental accuracy. Similarly, in cultured hepatocytes injected with fluorescently labelled dextran, repetitive bleaching had no systematic effect on the rate constant of nucleo-cytoplasmic flux (Peters, unpublished results).

Fluorescence microphotolysis may be employed for studying the permeability of the nuclear envelope within living cells. It is therefore instructive to discuss experiments of Cohen et al. (1971) dealing with this matter. The fluorescence of pyrimidine nucleotides was measured in small areas of single cells – either nucleus or cytoplasm – and glycolytic intermediates such as glucose 6-phosphate were injected either into the nucleus or into the cytoplasm. The time-lag between injection and fluorescence change was determined. If fluorescence was measured in the nucleus and injection performed at an average distance of s = 15 μm into the cytoplasm the time-lag was shorter than the instrumental time resolution of 35 ms. From these data we estimate the intracellular diffusion coefficient to be $D = s^2/6t = 1.0 \times 10^{-5}\,cm^2/s$. This value exceeds diffusion coefficients of comparable solutes in pure water. The diffusion coefficient of sucrose in water for instance is $5 \times 10^{-6}\,cm^2/s$. We assume that microinjection induces convection which – at least in normal-sized cells – effectively distributes the injected solute in the cell. Employing fluorescence microphotolysis we have recently measured solute transfer across the nuclear envelope in living hepatocytes (Peters, 1984). In these experiments microinjection was also employed. However, cells could be allowed to equilibrate after injection before flux measurements were started. Permeability measurements on living cells have benefits: the cell serves as cuvette and special procedures for arranging organelles in a thin layer are not required. Furthermore, outward-directed transport may be studied in addition to influx.

Appendix

Determination of rate constants and permeability coefficients from fluorescence measurements

As model a spherical vesicle of radius R, surface area A, and internal volume V is considered (Fig. 1B). The vesicle is suspended in an infinitely large compartment. The fluorescent solute is assumed to be uncharged and to penetrate the vesicle membrane by a passive, diffusional mechanism. At equilibrium, solute concentration c_e is equal in the external and internal phase. The sudden reduction of the concentration of fluorescent solute in the illuminated volume by a high-intensity light pulse triggers off a process involving diffusion in the external phase, permeation of the vesicle membrane, and diffusion in the internal phase. A theoretical description of solute transport under exactly these conditions is not available. However, a simpler system which sufficiently well approximates the actual case has been fully analysed. According to Fenichel and Horowitz (1969), solute transport from an infinitely large compartment into a sphere by both diffusion and membrane transport is completely membrane-limited, and external and internal phase are in diffusional equilibrium at all times if:

$$D \geq 10\,RP \tag{3}$$

where D is the diffusion coefficient of the solute and P is the membrane permeability coefficient. Even if $D = R\,P$ influx kinetics are still virtually single-exponential and, evaluated without taking diffusion into account, yield a 20% underestimation of P. As an example, an isolated liver cell nucleus of 4 μm radius may be considered: for a rather large permeability coefficient of 1×10^{-5} cm/s influx will be essentially membrane-limited as long as D is approximately $1 \times 10^{-9}\,cm^2/s$ or larger. Diffusion coefficients of proteins in water range from 10^{-7} to $10^{-6}\,cm^2/s$. In the cytoplasm, D-values are usually reduced by about 70%–95% (Paine and Horowitz 1980; Tanner 1983). Therefore, most flux measurements involving normal-sized cells are rate-limited by membrane permeation and diffusion can be neglected.

If membrane-permeation is rate-limiting, influx kinetics are simple and independent of vesicle geometry (for review of membrane transport theory see e.g., Sten-Knudsen 1978; Kotyk and Janáçek 1970). The derivation of the flux kinetics is trivial and Eqs. (4)–(7) are given here only for convenience. The flux dm/dt of solute across the membrane is

proportional to the concentration difference across the membrane:

$$dm/dt = A \cdot P \cdot \{c_e - c(t)\} \tag{4}$$

where $c(t)$ is the actual solute concentration in the internal phase at time t. Since $dm = V\, dc(t)$, Eq. (4) may be rearranged to yield:

$$\frac{1}{\{c_e - c(t)\}} dc = \frac{A \cdot P}{V} dt\,. \tag{5}$$

Setting $A \cdot P/V = k$ the relation between rate constant k and P is:

$$P = (V/A)k\,. \tag{6}$$

In case of a sphere $V/A = R/3$, for erythrocytes $V/A = 0.66$ μm (e.g., Kansu and Ersler 1980). Upon integration of Eq. (5) a frequently used flux equation is obtained:

$$\ln \frac{1}{\{c_e - c(t)\}} = \frac{1}{\{c_e - c(0)\}} + k \cdot t\,. \tag{7}$$

The measured fluorescence is largely determined by emission from the focal plane of the illuminated volume if light originating from other regions of the specimen is partially rejected by a diaphragm in an image plane in front of the photomultiplier (Koppel et al. 1976). This major fraction of the signal is denoted as $f(t)$ and is given by:

$$f(t) = 2\,\pi q \cdot c(t) \cdot \int_0^a I(r) r\, dr\,, \tag{8}$$

where q is the overall efficiency of fluorescence emission, collection and detection, $I(r)$ is the intensity of the illuminating beam, and a is the radius of the illuminated area ($a \leq R$, see Fig. 1). Equation (8) assumes that fluorescence is directly proportional to solute concentration and that the illumination intensity is constant in time (but may vary along the spatial coordinate, r). If an uniform profile of the illuminating beam is used, i.e.,

$$I(r) = \begin{cases} I_0 & \text{for } 0 \leq r \leq a \\ 0 & \text{for } r > a \end{cases} \tag{9}$$

integration of Eq. (8) yields:

$$f(t) = \pi a^2 \cdot q \cdot I_0 \cdot c(t)\,. \tag{10}$$

Equation 10 states that $f(t)$ is directly proportional to solute concentration. The same holds for any intensity profile because in Eq. (8) evaluation of the integral yields a constant factor for any $I(r)$. For the same reason a direct proportionality of measuring signal and $c(t)$ is also given for regions of the specimen which are out of focus and which, although to a minor degree, may contribute to the total measuring signal denoted as $F(t)$.

Since $F(t)$ is proportional to $c(t)$ Eq. (8) can be rewritten by replacing c_e by F_e, the equilibrium fluorescence, $c(0)$ by $F(0)$, the fluorescence shortly after photolysis when diffusional equilibrium has been reached but influx justs starts, and $c(t)$ by $F(t)$. In the simplest case the equilibrium fluorescence F_e is equal to both fluorescence $F(-)$ before photolysis, and fluorescence $F(\infty)$ very long after photolysis. However, adsorption to the membrane can result in an immobilization of part of the solute. In that case $F(\infty)$ is smaller than $F(-)$. Therefore, as the general case, the time-course of influx is given by Eq. (1).

If the illuminated area is larger than the vesicle ($a > R$) $f(t)$, in case of an uniform intensity profile, is:

$$\begin{aligned} f(t) &= 2\,\pi q \cdot I_0 \cdot \{c(t) \cdot \int_0^R r dr + c_e \int_R^a r dr\} \\ &= \pi q \cdot I_0 \cdot \{c(t) R^2 + c_e(a^2 - R^2)\}\,. \end{aligned} \tag{11}$$

In Eq. (11) the time-dependent component is not a function of a, the radius of the illuminated area. However, a time-independent term is present, which depends on a and, with increasing a, tends to dominate the fluorescence signal. This effect is more clearly apparent if the ratio $F(0)/F(\infty)$ is considered. Simple rearrangements show that:

$$\frac{F(0)}{F(\infty)} = \left\{\frac{c(0)}{c_e} - 1\right\}\left\{\left(\frac{R}{a}\right)^2 + 1\right\}. \tag{12}$$

Curve fitting

Equation (1) suggests plotting the data as $\ln[1/F(\infty)\text{-}F(t)]$ versus t. It is, however, not convenient to extend measurements to "infinite" time. Therefore, we have used a computer program (Meller and Peters, unpublished results) which performs the following operations. Data evaluation is started by setting $F(\infty) = F(-)$ and plotting in $\ln[1/F(-)\text{-}F(t)]$ versus time. A linear regression analysis is performed and the reduced chi-square computed as a measure of linearity. Then, $F(\infty)$ is varied and the regression analysis repeated until the optimum $F(\infty)$-value yielding the smallest chi-square is found. The best fit is used to derive $F(\infty)$, $F(0)$, k,P, and R_M, the mobile fraction.

Acknowledgements. Support by the Deutsche Forschungsgemeinschaft is gratefully acknowledged.

References

Axelrod D (1977) Cell surface heating during fluorescence photobleaching recovery experiments. Biophys J 18: 129–131

Axelrod D (1983) Lateral motion of membrane proteins and biological function. J Membr Biol 75: 1–10

Axelrod D, Koppel DE, Schlessinger J, Elson E, Webb WW (1976) Mobility measurements by analysis of fluorescence photobleaching recovery experiments. Biophys J 16: 1055–1069

Cherry RJ (1979) Rotational and lateral diffusion of membrane proteins. Biochim Biophys Acta 559: 289–327

Christensen HN (1975) Biological transport. Benjamin, Reading

Davoust J, Devaux PF, Leger L (1982) Fringe pattern photobleaching, a new method for the measurement of transport coefficients of biological macromolecules. EMBO J 1: 1233–1238

Dodge JT, Mitchell C, Hanahan, DJ (1963) The preparation and chemical characterization of hemoglobin-free ghosts of human erythrocytes. Arch Biochem Biophys 100: 119–130

Edidin M, Zagyanski Y, Lardner TJ (1976) Measurement of membrane lateral diffusion in single cells. Science 191: 466–468

Eidelman O, Cabantchik ZI (1980) A method for measuring anion transfer across red cell membranes by continuous monitoring of fluorescence. Anal Biochem 106: 335–341

Fenichel RI, Horowitz SB (1969) Intracellular transport. In: Dowben RM (ed) Biological membranes. Little, Brown and Company, Boston, pp 177–221

Halestrap AP, McGivan JD (1979) Measurement of membrane transport phenomena. Tech Metabol Res B206: 1–23

Jacobson K, Wu E, Poste G (1976) Measurement of the translational mobility of concanavalin A in glycerol-saline solutions and on the cell surface by fluorescence recovery after photobleaching. Biochim Biophys Acta 43: 215–222

Jacobson K, Hou Y, Wojcienszyn J (1978) Evidence for lack of damage during photobleaching measurements of lateral mobility of cell surface components. Exp Cell Res 116: 179–189

Johnson P, Garland PB (1981) Depolarization of fluorescence depletion. A microscopic method for measuring rotational diffusion of membrane proteins on the surface of a single cell. FEBS Lett 132: 252–256

Kansu E, Ersler AJ (1980) The red cell. In: Seligson D (ed) Clinical laboratory science, vol 2. CRC Press, Boca Raton, Sect 1, pp 123–142

Kohen E, Siebert G, Kohen C (1971) Transfer of metabolites across the nuclear membrane Hoppe-Seyler's. Z Physiol Chem 352: 927–937

Koppel DE (1979) Fluorescence redistribution after photobleaching: a new multipoint analysis of membrane translational dynamics. Biophys J 28: 281–292

Koppel DE (1983) Fluorescence photobleaching as a probe of translational and rotational motions. In: Sha'afi RI, Fernandez SM (eds) Fast methods in physical biochemistry. Elsevier, Amsterdam New York Oxford, pp 339–367

Koppel DE, Axelrod D, Schlessinger J, Elson EL, Webb WW (1976) Dynamics of fluorescence marker concentration as a probe of mobility. Biophys J 16: 1315–1329

Kotyk A, Janáçek K (1970) Cell membrane transport. Plenum Press, New York London

Lanni F, Ware BR (1982) Modulation detection of fluorescence photobleaching recovery. Rev Sci Instrum 53: 905–908

Lieber MR, Steck TL (1982) A description of the holes in human erythrocyte membrane ghosts. J Biol Chem 257: 11651–11659

Nigg EA, Kessler M, Cherry RJ (1979) Labeling of human erythrocyte membranes with eosin probes used for protein diffusion measurements: inhibition of anion transport and photooxidative inactivation of acetylcholinesterase. Biochim Biophys Acta 550: 328–340

Paine PL, Horowitz SB (1980) The movement of material between nucleus and cytoplasm. In: Goldstein L, Prescott DM (eds) Cell biology, vol 4. Academic Press, New York, pp 299–341

Parker CA (1968) Photoluminescence in solution. Elsevier, Amsterdam London New York

Pfaff E, Klingenberg M (1968) Adenine nucleotide translocation of mitochondria. Eur J Biochem 6: 66–79

Peters R (1981) Translational diffusion in the plasma membrane of single cells as studied by fluorescence microphotolysis. Cell Biol Int Rep 5: 733–760

Peters R (1983a) Fluorescence microphotolysis. Diffusion measurements in single cells. Naturwissenschaften 70: 294–302

Peters R (1983b) Nuclear envelope permeability measured by fluorescence microphotolysis of single liver cell nuclei. J Biol Chem 258: 11427–11429

Peters R (1984) Nucleo-cytoplasmic flux and intracellular mobility in single hepatocytes measured by fluorescence microphotolysis. EMBO J (in press)

Peters R, Richter HP (1981) Translational diffusion in the plasma membrane of sea urchin eggs. Dev Biol 86: 285–293

Peters R, Peters J, Tews KH, Bähr W (1974) A microfluorimetric study of translational diffusion in erythrocyte membranes Biochim Biophys Acta 367: 282–294

Peters R, Brünger A, Schulten K (1981) Continuous fluorescence microphotolysis: A sensitive method for the study of translational diffusion in single cells. Proc Natl Acad Sci USA 778: 962–966

Schulz SG (1980) Basic principles of membrane transport. Cambridge University Press, Cambridge London New York Melbourne Sydney

Sheetz MP, Koppel DE (1979) Membrane damage caused by irradiation of fluorescent concanavalin A. Proc Natl Acad Sci USA 76: 3314–3317

Sims PJ, Waggoner AS, Wang CH, Hoffman JF (1974) Studies on the mechanism by which cyanine dyes measure membrane potential in red blood cells and phosphatidylcholine vesicles. Biochemistry 13: 3315–3330

Smith BA, McConnell HM (1978) Determination of molecular motion in membranes using periodic pattern photobleaching. Proc Natl Acad Sci USA 75: 2759–2763

Smith LM, Weis RM, McConnell HM (1981) Measurement of rotational diffusion of membrane components by fluorescence photobleaching. Biophys J 36: 73–91

Sten-Knudsen O (1978) Passive transport processes. In: Giebisch G, Tosteson DC, Ussing HH (eds) Membrane transport in biology, vol 4. Springer Verlag, Berlin Heidelberg New York, p 5113

Tanner JE (1983) Intracellular diffusion of water. Arch Biochem Biophys 224: 416–428

Thompson NL, Burghardt TP, Axelrod D (1981) Measuring surface dynamics of biomolecules by total internal reflection fluorescence with photobleaching recovery or correlation spectroscopy. Biophys J 33: 435–454

Vaz WLC, Derzko ZI, Jacobson KA (1982) Photobleaching measurements of the lateral diffusion of lipids and proteins in artificial phospholipid bilayer membranes. In: Poste G, Nicolson GL (eds) Membrane reconstitution. Elsevier, Amsterdam New York Oxford, pp 83–136

Wohlhueter RM, Marz R, Graff JC, Plagemann PWG (1978) A rapid-mixing technique to measure transport in suspended animal cells: Applications to nucleoside transport in Novikoff rat hepatoma cells. Methods Cell Biol 20: 211–236

Wolf DE, Edidin M, Dragsten PR (1980) Effect of bleaching light on measurements of lateral diffusion in cell membranes by the fluorescence photobleaching recovery method. Proc Natl Acad Sci USA 77: 2043–2045